AD-A054 477 MASSACHUSETTS INST OF TECH LEXINGTON LINCOLN LAB F/G 20/6
ELECTROOPTICAL DEVICES.(U)
SEP 77 I MELNGAILIS, A G FOYT F19628-76-C-0002

UNCLASSIFIED ESD-TR-78-28 NL

| OF |
AD
A054477

END
DATE
FILMED
6-78
DDC

MASSACHUSETTS INSTITUTE OF TECHNOLOGY

LINCOLN LABORATORY

(6) ELECTROOPTICAL DEVICES

(9) SEMIANNUAL TECHNICAL SUMMARY REPORT, 1 Apr – 30 Sep 77

TO THE

ROME AIR DEVELOPMENT CENTER

(10) Ivars Melngailis Arthur G. Foyt, Jr

(15) F19628-76-C-0002

(16) 2611 (17) 04

(11) 1 APRIL – 30 SEP 1977

(12) 27 p.

ISSUED 28 MARCH 1978

(18) ESD (19) TR-78-28

Approved for public release; distribution unlimited.

LEXINGTON MASSACHUSETTS

ABSTRACT

Considerable progress has been made toward the achievement of the current objectives of the electrooptical device program. These goals are: (1) to perform life tests on GaInAsP/InP double-heterostructure (DH) diode lasers operating in the 1.0- to 1.3-μm wavelength region and analyze the degradation mechanisms, and (2) to fabricate and study avalanche photodiodes of similar composition GaInAsP operating in the same wavelength region.

Life tests of CW, room-temperature GaInAsP/InP DH lasers have continued with a total of 13 devices examined in some detail. Eleven of the lasers have operated for over 2000 hours, with the longest-lived operating 7700 hours before failure. End-face contamination problems have apparently been reduced and other mechanisms for degradation, both of external and internal nature, are under study.

CW operation of the DH GaInAsP/InP lasers has been demonstrated at temperatures up to 50°C. The pulsed threshold was found to increase with temperature as $J_{th} = J_o \exp(T/T_o)$ with $T_o \approx 75°C$ and J_o a constant. Over the temperature range $10°C < T < 50°C$, the temperature dependence of the wavelength was approximately linear with $\Delta\lambda/\Delta T \approx 3.2$ Å/°C.

The pulse response and modulation characteristics of GaInAsP/InP lasers have also been investigated. Clean output pulses with risetimes of less than 250 psec, pulse modulation at 200 megapulses/sec, and pulse-position modulation at a 100-Mbit/sec rate have been achieved. Modulation rates in the GHz range should be attainable.

Avalanche diodes with response from 0.9 to 1.3 μm have been successfully fabricated in GaInAsP/InP double-heterostructure configurations. Uniform avalanche gains in excess of 12, risetimes of 200 psec or less, and low bias quantum efficiencies of 45 percent have been measured.

Implantation of ions of Se^+ and Si^+ has been used to create n-type layers in InP. With both ions, sheet resistivities of 15 to 16 Ω/□ have been achieved with electrical activations of nearly 80 percent over a wide range of doses. P-type layers were created with Cd^+, Mg^+, and Be^+, with initial studies concentrating on the effects of varying implant and anneal temperatures. Diffusion of these p-type dopant ions during annealing has been found to be more rapid than expected.

Studies of the implantation of Fe^+ shows that high-resistivity layers ($\rho \geq 10^7$ Ω-cm) can be created in n-type InP. Depth profiles indicate a relatively rapid diffusion of the Fe during anneal. An apparent anomalous donor peak at the edge of the high-resistivity region has been tentatively explained by a model involving the charging and discharging of the Fe levels.

CONTENTS

ELECTROOPTICAL DEVICES

I. GaInAsP/InP DOUBLE-HETEROSTRUCTURE LASERS

A. LIFE TESTS OF GaInAsP/InP LASERS

Life tests of CW, room-temperature GaInAsP/InP double-heterostructure diode lasers have continued, with a total of 13 devices examined in some detail. Of these, three are the original lasers discussed in the previous report,[1] and the remaining ten are similar devices. The latter devices were operated under carefully controlled heat sink temperature (±0.1°C) and current (±2 mA) conditions in the test setup described previously.[1]

For lasers operated at room temperature with a fixed current, the typical power output as a function of operating time for two devices is shown in Fig. I-1. It is clear that, even with careful control of device current and heat-sink temperature, substantial variations in output power vs time are observed prior to the device end of life. Comparative lifetime characteristics of the lasers are being studied by operating them CW with the current adjusted to an initial output power of 2 to 4 mW per facet.

For the devices under constant current operation, the lifetime is arbitrarily defined as the operating time at which the output power drops below 1 mW. A histogram of the lifetime data so obtained on 13 devices is shown in Fig. I-2. Lifetimes ranged from a few hundred to 7500 hours, with two devices still operating at the present time.

For most of the lasers which have failed, end-face degradation has been identified as the primary cause of failure. In fact, it was usually possible to restore the output of degraded lasers to nearly original values by rinsing the devices in a buffered HF solution. The degradation-restoration cycle could be repeated several times before the end faces became irreversibly degraded. This problem has been the focus of attention during this past six-month period. Avenues of investigation have included:

(1) Thorough device cleaning at several stages in the fabrication processing, including use of detergents, organic solvents, and acid washes.

(2) Study of different fluxes for indium solder bond of device to heat sink.

(3) Protective coatings for laser end faces.

It appears that beneficial effects can be obtained both by the use of a sputtered Al_2O_3 protective coating and by careful cleaning with an acid solution. These techniques are being evaluated in detail at present and, as a solution to the facet contamination problem is realized, studies of device lifetime and of mechanisms for degradation at both room and elevated temperatures will be continued and expanded.

C. C. Shen
J. J. Hsieh
T. A. Lind

B. CW OPERATION OF GaInAsP/InP LASERS UP TO 50°C

In this section, we report the CW operation of double-heterostructure (DH) $Ga_xIn_{1-x}As_yP_{1-y}$ lasers ($x = 0.21$, $y = 0.50$) at heat-sink temperatures up to 50°C. The lasers are proton-defined stripe-geometry devices similar to those reported on previously.[1] The active region thickness

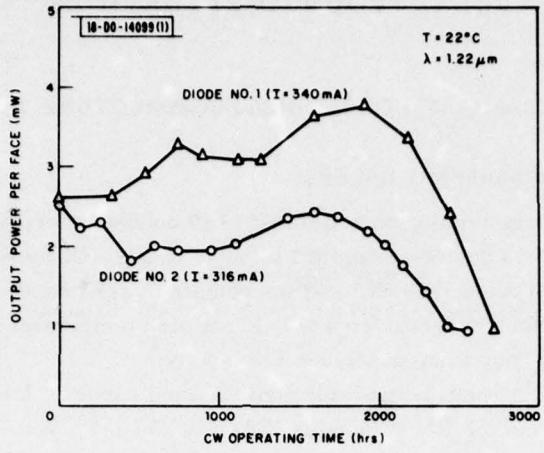

Fig. I-1. Output power vs CW operating time for two GaInAsP/InP double-heterostructure (DH) lasers running at room temperature.

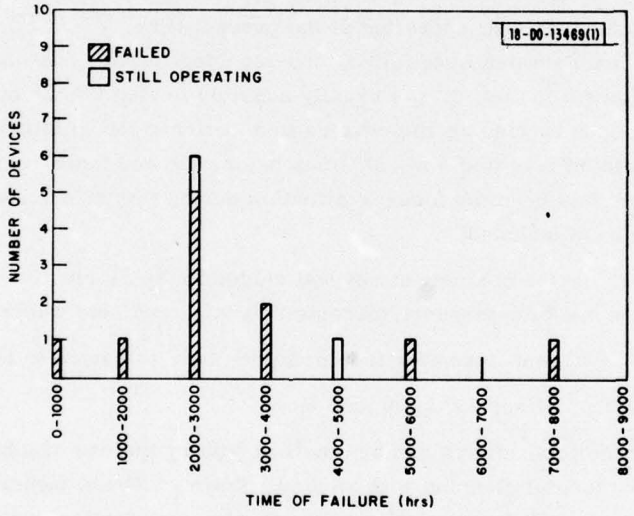

Fig. I-2. Histogram of lifetime data on 13 GaInAsP/InP DH lasers operating CW at room temperature.

is about 0.2 μm, the stripe width 13 μm, and the cavity length typically 380 to 400 μm. Emission is at 1.22 μm at 22°C. The total series resistance of the devices is typically 2 to 3 ohms.

For pulsed operation, the diodes were mounted on a testing jig and driven with low-duty-cycle (100-nsec and 75-pps) pulses. The light output was detected with a Ge avalanche photodiode and displayed on a fast oscilloscope. The lasing spectrum was obtained by focusing the light into a grating spectrometer and detecting the radiation with a cooled S-1 photomultiplier.

A room-temperature threshold current density as low as 4.4 kA/cm^2 was obtained. The total variation in J_{th} for devices fabricated from the same wafer was less than 50 percent. To study the threshold characteristics at different heat-sink temperatures, individual lasers were mounted with p-side down in diode packages using In solder. A diode package was then attached to a copper heat sink where temperature was varied by a thermoelectric cooling and heating device. In Fig. I-3, we plot the pulsed threshold current density vs the heat-sink temperature T for 0°C < T < 50°C. The threshold current, J_{th}, increases exponentially with T and can be described by $J_{th} \approx J_o \exp(T/T_o)$ where $T_o \sim 75$°C and J_o is a constant.

In CW operation, diodes were driven with a constant-current source. The light output from one facet of a laser was coupled into an optical fiber and detected at the other end with a calibrated Ge photodiode. In Fig. I-4, the laser output power is plotted vs operating current for several heat-sink temperatures from 22°C to 50°C. The differential quantum efficiency is

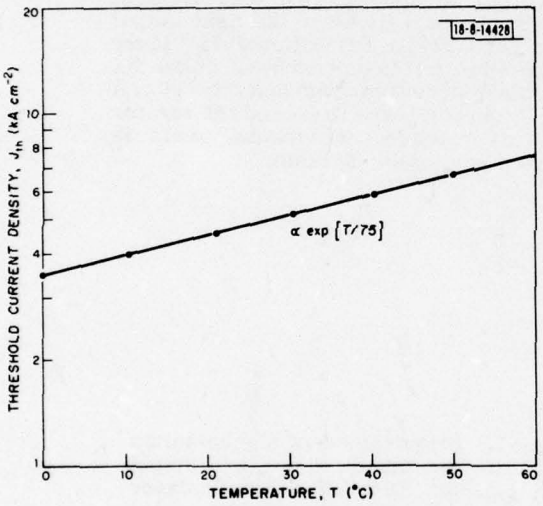

Fig. I-3. Threshold current density vs heat-sink temperature for a DH GaInAsP/InP laser emitting at 1.22 μm.

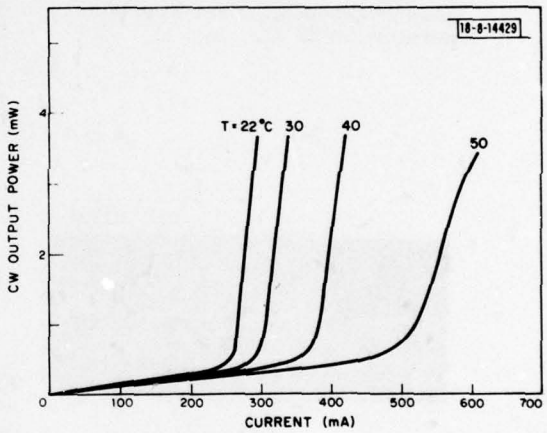

Fig. I-4. CW output power per face vs operating current at different heat-sink temperatures for a DH GaInAsP/InP laser.

10 percent per face from 22° up to 40°C, then drops to 3.6 percent as T is raised to 50°C because of severe joule heating at high operating current. A typical CW emission spectrum at threshold consists of a large number of longitudinal modes which cover a band about 250 to 300 Å wide. The spectrum narrows to only a few longitudinal modes as the pumping current increases to 5 to 10 percent above threshold. In some cases, a single mode is observed. Figure I-5 shows the emission spectrum for a laser operating at 10 percent above threshold. The

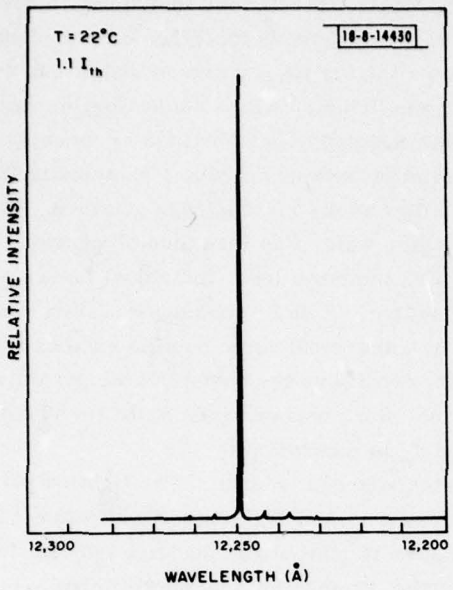

Fig. I-5. CW emission spectrum for a DH GaInAsP/InP laser operating at 320 mA (10 percent above threshold). Heat-sink temperature is 22°C.

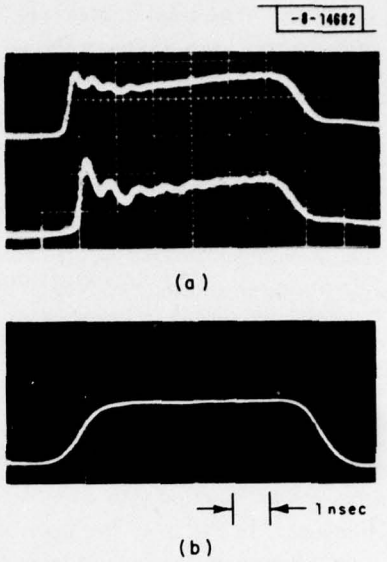

Fig. I-6. Response (a) of a germanium avalanche photodiode to the light output of a DH 1.22-μm DH GaInAsP/InP laser driven by the 50-mA current pulse (b). DC bias current through laser is 300 mA for the upper trace in (a) and 285 mA for the lower trace. Horizontal scale is 1 nsec per major division.

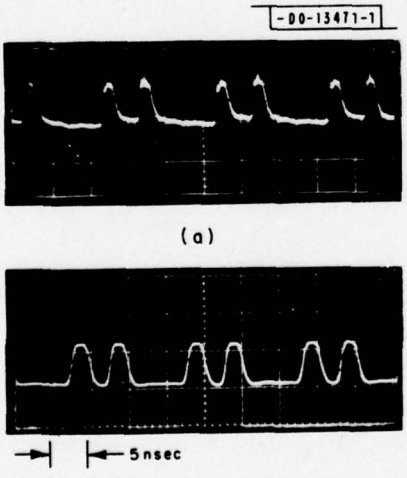

Fig. I-7. Response (a) of a germanium avalanche photodiode to the light output of a 1.22-μm DH GaInAsP/InP laser driven by the 25-mA current pulse train (b). The laser was biased at threshold (260 mA). Time scale is 5 nsec per major division.

temperature dependence of the lasing wavelength λ was investigated by operating the device in the pulsed mode at a controlled heat-sink temperature T. It was found that λ increased linearly with T for $10°C < T < 50°C$ with $\Delta\lambda/\Delta T \sim 3.2$ Å/°C.

C. C. Shen
J. J. Hsieh
T. A. Lind

C. PULSE RESPONSE AND MODULATION CHARACTERISTICS OF GaInAsP/InP LASERS

Initial results of pulse response and modulation experiments of GaInAsP/InP lasers have been most encouraging. Clean, fast-risetime output pulses and 200-megapulse/sec modulation have been achieved.

The measurements were performed on stripe geometry lasers identical to those described in a previous report.[1] The stripe widths and cavity lengths were 13 μm and 380 μm, respectively, and the devices had threshold current densities at room temperature of about 5 kA/cm^2 pulsed and 6 kA/cm^2 CW. A bias-tee arrangement was employed so that a DC bias current could be supplied simultaneously with the drive pulse. Variable width pulses with 1 nsec rise and fall time were used in these experiments. The laser output was observed with a germanium avalanche photodiode operating into the 50-Ω input of a sampling oscilloscope.

Oscilloscope traces of the input current pulse and the detector response to the laser output are shown in Fig. I-6 for two different DC bias levels on the laser. The laser threshold current was 300 mA, so that the two bias levels of 285 mA and 300 mA correspond to below and just at threshold, respectively. The current pulse had an amplitude of 50 mA.

In both cases, the observed risetime is approximately 250 psec, a value which is about the same as that measured by Yamamoto et al.[2] for a GaInAsP/InP laser with no DC bias. When the DC is well below threshold, the pulsed laser output exhibits the characteristic damped relaxation oscillation of these, as well as a GaAs/AlGaAs laser. However, when the DC bias is just below or at threshold, the ringing is minimized and a relatively clean output pulse is obtained as in Fig. I-6.

To determine the suitability of the lasers for pulse modulated sources, they were driven with 2-nsec pulses at 200 megapulses/sec, as well as with pairs of similar pulses to simulate 100-Mbit/sec pulse-position modulation. The results of the latter experiment are shown in Fig. I-7. Clearly the modulation capabilities of these lasers are well in excess of the rates used. Indeed, it has been estimated by Yamamoto et al.[2] that modulation frequencies of a few GHz should be achievable.

C. C. Shen
A. G. Foyt

II. GaInAsP/InP AVALANCHE PHOTODIODES

Avalanche multiplication of a photosignal has been observed for the first time in diodes of the quaternary alloy GaInAsP. The diodes, which were fabricated from quaternary layers lattice-matched to InP substrates, had a long-wavelength cutoff of 1.25 μm. Diodes having a response cutoff out to 1.6 μm are possible in this quaternary system with compositions still lattice-matched to InP. Avalanche diodes in the GaInAsP material system are expected to have important applications in the fields of fiber optics communications and integrated optical circuits. Recently, avalanche multiplication at 1.2 μm in the ternary alloy GaInAs, lattice-matched to an InP substrate, as well as normal photodiode operation in GaInAsP have been reported in the literature.[3,4]

Multiplication has been observed in the two similar etched mesa diode structures shown schematically in Fig. II-1. In both cases, the quaternary and top InP layers were grown by

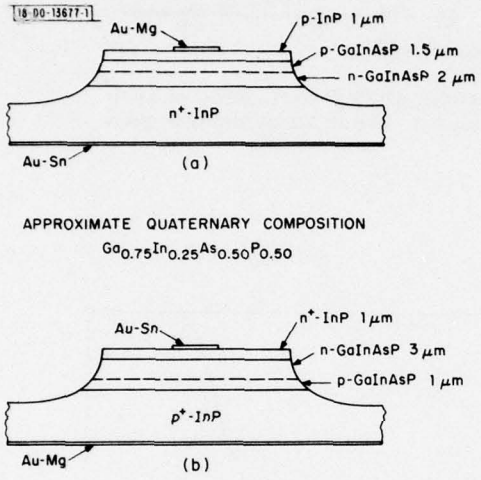

Fig. II-1. Schematic diagram of normal (a) and inverted (b) mesa GaInAsP/InP photodiode structures.

liquid-phase epitaxy (LPE) on InP substrates, with the nominal composition of the quaternary layers in the two structures being $Ga_{0.75}In_{0.25}As_{0.50}P_{0.50}$. In the structure shown in Fig. II-1(a), the quaternary capping InP layers were initially undoped ($n \approx 1$ to 3×10^{16} cm^{-3}) and the p-n junction was formed by diffusing Zn (an acceptor) through the top InP layer into the GaInAsP. C-V measurements indicated that the junction was graded over a range of 1.9 μm, with the net donor concentration increasing from 8×10^{15} cm^{-3} at the zero-bias depletion layer edge to 2×10^{16} cm^{-3}, a value characteristic of the as-grown layer. This shape of graded layer presumably corresponds to that of the Zn diffusion front.

Mesas of 150-μm diameter were etched using 1% Br in methanol or a 1:6:1:1 solution of $HCl:HNO_3:HAc:HClO_4$. Contacts of evaporated Au-Mg (p-type) and plated Au-Sn (n-type) were alloyed at 400°C. Breakdown voltages of the diodes were in the 50- to 60-V range. The spectral response of one of the devices with and without bias is shown in Fig. II-2. Illumination was from the direction of the top contact, although the transparent InP substrate and top layer will permit illumination from either direction. This feature will be highly useful in future experiments to measure electron and hole ionization rates. The observed signal increase with bias corresponds to an avalanche gain of about four. The shift of the response cutoff to longer wavelengths at the

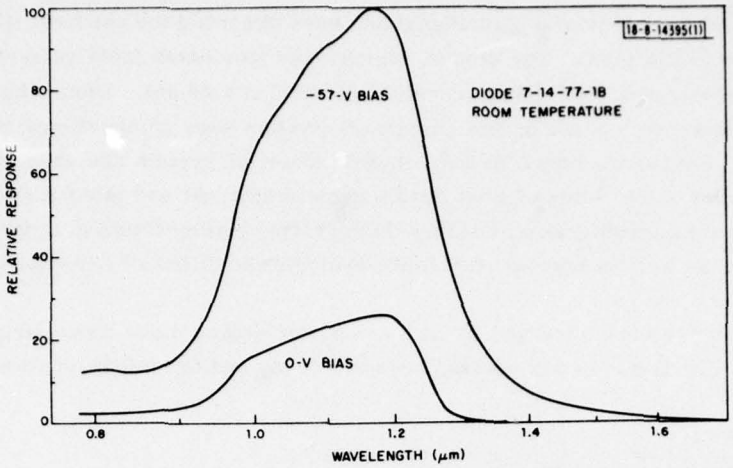

Fig. II-2. Spectral response of a GaInAsP/InP photodiode at zero bias and with sufficient reverse bias to cause an avalanche gain of about four.

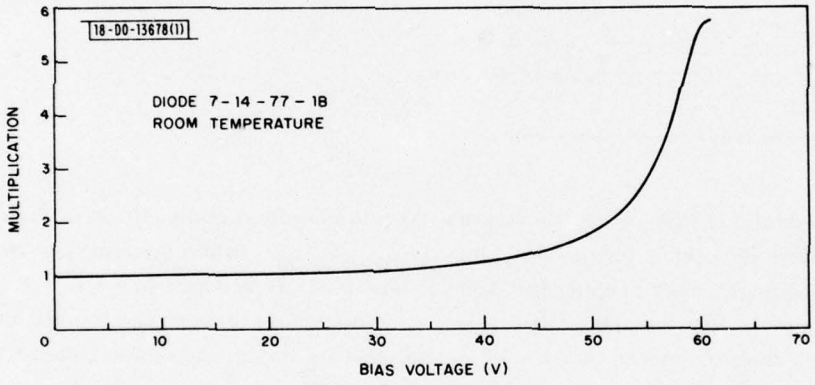

Fig. II-3. Multiplication vs applied bias for the same diode as in Fig. II-2. Excitation wavelength was 1.17 μm.

higher bias is presumably due to the Franz-Keldysh effect, as has been observed in GaAs avalanche diodes.[5] Figure II-3 shows the multiplication vs applied voltage for the same diode with 1.17-μm excitation.

The uniformity of response of the devices was also examined with a raster-scanned focused spot from a 1.15-μm GaInAsP/InP laser. The response was quite uniform up to biases yielding a gain of four or five. For higher reverse voltages, there was a rapid increase in multiplied signal at the edge of the mesa, indicating the onset of edge breakdown. This behavior is to be expected from the normal mesa geometry because of the higher field at the junction periphery due to field crowding.

To reduce the gain limitation due to edge breakdown, the inverted mesa structure shown in Fig. II-1(b) was fabricated and tested. As in the normal mesa structure, the GaInAsP layer was not intentionally doped and the p-n junction was formed by diffusion of Zn, this time by outdiffusion from the heavily Zn-doped InP substrate. Contacts were applied and mesas etched as before. Again, the C-V measurements indicated a graded junction with characteristics similar to those described above. However, these diodes had somewhat higher breakdown voltages (65 to 70 V), showed no evidence of edge multiplication, and gave somewhat higher values of gain (as high as 12). A typical I-V characteristic for one of the devices is shown in Fig. II-4.

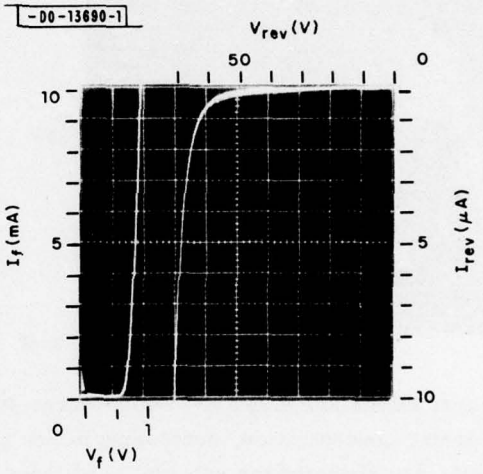

Fig. II-4. Forward and reverse I-V characteristics of a typical inverted-mesa device.

Raster scans of the diode response at 1.15 μm for conditions of no gain and for a gain of about eight are shown in Fig. II-5. For higher biases, the multiplication appears to be limited by microplasma breakdown and/or by excess leakage current, possibly at the unpassivated surface.

Initial measurements of the low bias quantum efficiency and speed of response of the diodes were also made. The quantum efficiency at 1.15 μm was approximately 45 percent. When biased to yield a gain of about eight, the risetime of the avalanche diode response to a pulse from a GaInAsP/InP laser was less than 200 psec. At present, we have not determined whether the observed risetime is characteristic of the laser or detector.

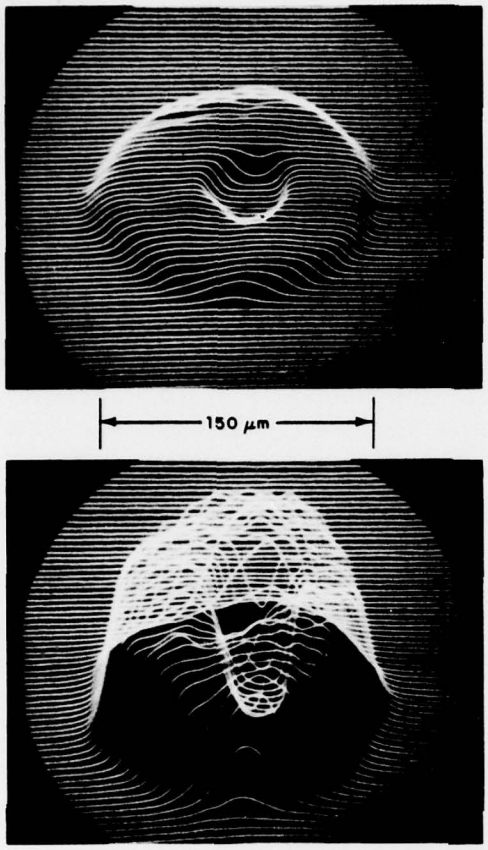

Fig. II-5. Raster scans at 1.15-μm excitation of a 150-μm-diameter inverted mesa avalanche diode. Scan (a) is at a bias of 24 V and little or no gain ($M \approx 1$). Scan (b) is at a reverse voltage of 71.8 V and corresponds to a multiplication (M) of about eight.

Present experiments are directed toward increasing the attainable multiplication by lowering the GaInAsP carrier concentration, developing better guard-ring techniques, eliminating surface leakage currents, and reducing the substrate and layer dislocation densities to reduce microplasmas. Measurements of device noise performance and electron and hole ionization rates as well as more refined speed and quantum efficiency measurements will also be made.

C. E. Hurwitz
J. J. Hsieh
R. L. Payer

III. ION IMPLANTATION IN InP

A. N- AND p-TYPE ION IMPLANTED LAYERS IN InP

Ion implantation in InP has the potential of being of significant practical importance in the fabrication of optoelectronic and microwave devices. Although implantation of Si^+ and Se^+ in $InAs_xP_{1-x}$ ($x \geq 0.2$) has been reported,[6] there has been little published work on ion implantation in InP. In our last report,[7] we gave a brief summary of our initial results in this area. In this section, we report in more detail our results on the use of ion implantation to creat both n- and p-type layers in InP. Ions of Se^+ and Si^+ implanted at 400 keV were used to make n-type layers, while p-type layers were made with Be^+, Mg^+, and Cd^+ ions implanted at 50, 150, and 400 keV, respectively. Some implantations of Kr^+ were also made to investigate the nature of the residual implantation-induced damage. An encapsulation technique using pyrolytic phosphosilicate glass (PSG) was developed to reproducibly protect the sample at the required 700° to 750°C annealing temperatures.

The InP samples used in these experiments were cut from (111)-oriented crystals, polished and etched[8] in a 1:1:6:1 mixture of $HAc:HClO_4:HNO_3:HCl$. During implantation, they were held at either 77 K, room temperature, or 200°C, and were tilted with reference to the ion beam to minimize channelling. Prior to annealing, the samples were encapsulated with 2500 to 3000 Å of pyrolytic phosphosilicate glass (PSG) deposited at 250°C. Other coatings including pyrolytic SiO_2 and sputtered and pyrolytic Si_3N_4 were tried, but they generally cracked and/or peeled at temperatures above 700°C. The PSG was deposited in a "cold wall" reactor similar to that used to deposit pyrolytic silicon nitride.[9-11] Two inlet lines were used, one carrying 400 scc/min. of 0.2% PH_3 in N_2 and 125 scc/min. of 15% SiH_4 in N_2 further diluted in 4000 scc/min. of N_2, and the other carrying 140 scc/min. of O_2 diluted in 4000 scc/min. of N_2. After the flows reached a steady state, the InP was heated rapidly by means of a low-mass graphite heater strip to 250°C to initiate deposition of the PSG. It took approximately 3-1/2 min. to deposit 2500 Å of PSG, after which the sample was rapidly cooled. The composition of the PSG was determined by wet chemical analysis to be nominally 7.84 wt percent P (17.96 wt percent P_2O_5), for which composition the thermal expansion coefficient has been reported[12] to be about 3.4×10^{-6}/°C, as compared to 4.5×10^{-6}/°C for InP.

Annealing was carried out in flowing nitrogen at temperatures of 700° to 750°C for 1 to 15 min. It was found that anneal times of 5 to 15 min. gave the same results. Microalloyed plated Au-Sn was used to contact n-type layers while microalloyed evaporated Au-Zn or Au-Mg was used to contact the p-type regions. Cloverleaf patterns were then etched in the implanted layers to facilitate Hall measurements of the van der Pauw type.[13]

To test the effectiveness of the PSG encapsulation on the InP, some annealing experiments were performed on unimplanted samples of high-resistivity ($\rho \geq 10^7$ Ω-cm) Fe-doped InP. As in high-resistivity Cr-doped GaAs,[14] variations in annealing results among samples from different ingots of the Fe-doped InP were observed. For crystal 25RH, unimplanted samples were either coated with PSG directly after etching or first heated to 200°C in the implantation system to duplicate the conditions of a hot implant. In either case, 15-min. anneals at temperatures up to 750°C produced no measurable conducting layers on the unimplanted samples. Following a 775°C anneal, however, n-type surface layers with sheet electron concentrations of 2×10^{11} cm^{-2} were observed. Samples from another crystal, HPOZ9, when heated to

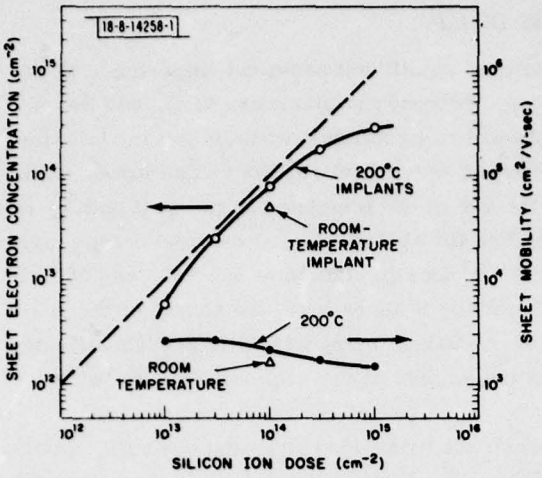

Fig. III-1. Sheet electron concentration and mobility vs dose for 400-keV Si^+-implanted Fe-doped InP crystal 25RH. The samples were implanted bare, encapsulated with PSG, and annealed at 750°C for 15 min.

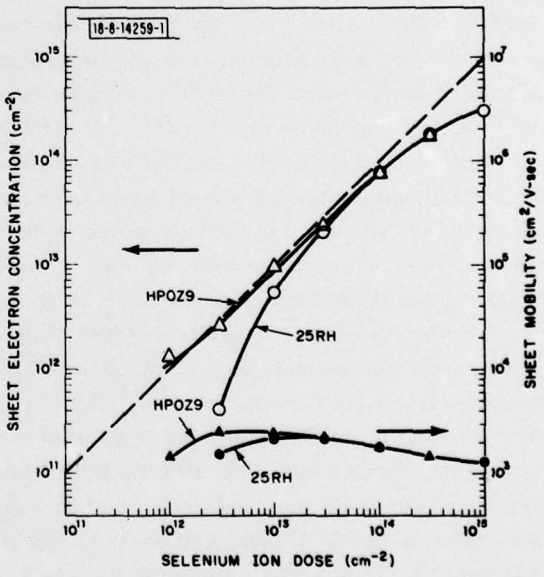

Fig. III-2. Sheet electron concentration and mobility vs dose for two different Fe-doped InP ingots implanted with 400-keV Se^+ ions. The samples were implanted bare, encapsulated with PSG, and annealed at 750°C for 15 min.

200°C and then encapsulated and annealed at 750°C for 15 min., had n-type skins with $n \approx 4 \times 10^{11}$ cm^{-2}. As discussed below, this latter crystal also behaved somewhat differently for low-dose Se^+ implants.

To assess the possible effects of residual damage on the implantation, 400-keV Kr^+ ions were implanted into Fe-doped InP crystal 25RH. On samples implanted with 1×10^{12} cm^{-2} Kr^+ at either room temperature or 200°C and annealed at 750°C, there were no measurable conducting surface layers. For samples implanted with 1×10^{14} cm^{-2} Kr^+ and annealed at 750°C, however, n-type surface layers with concentrations of (4 to 6) $\times 10^{12}$ cm^{-2} were observed when the implant was carried out at room temperature, while concentrations of only (0.6 to 3) $\times 10^{11}$ cm^{-2} were observed when the implants were carried out at 200°C. The sheet concentrations measured on the samples annealed at 750°C were much lower than those observed on unannealed samples and were also generally lower than those on samples annealed at 700° and 725°C. From these results, it appears that residual damage in InP is n-type and, at least for heavy ions, this n-type damage can be reduced substantially by implanting at 200°C. In recent experiments, however, there is some indication that some damage-enhanced diffusion or decomposition may take place during a 200°C implant. There may therefore be an optimum implant temperature between room temperature and 200°C which minimizes the formation of n-type skins with heavy ion bombardment.

Implantations of the donor ions Si^+ and Se^+ were performed with substrates at room temperature and 200°C. For a dose of 1×10^{14} cm^{-2} of either ion, higher sheet carrier concentrations, N_s, and mobilities, μ_s, were obtained for the higher temperature implants. With Se (the experiments were not performed for Si^+), both parameters also increased with increasing anneal temperature between 700° and 750°C. For samples implanted with 1×10^{14} cm^{-2} Se at room temperature, N_s and μ_s were 4.8×10^{13} cm^{-2} and 1170 cm^2/V-sec, respectively, following a 700°C anneal, and 6.0×10^{13} cm^{-2} and 1470 cm^2/V-sec, respectively, following a 750°C anneal. For similar samples implanted at 200°C, N_s and μ_s were 6.9×10^{13} cm^{-2} and 1710 cm^2/V-sec, respectively, following a 700°C anneal, and 7.9×10^{13} cm^{-2} and 1810 cm^2/V-sec, respectively, following a 750°C anneal.

Figure III-1 shows the measured sheet carrier concentration and mobility vs Si^+ ion dose for Fe-doped InP samples (25RH) implanted at 200°C and annealed at 750°C for 15 min. For comparison, the results of a room-temperature 1×10^{14} cm^{-2} Si implant are also shown. The dashed line represents 100-percent electrical activation of the implanted silicon. The highest measured activation of 80 percent was obtained for a dose of 3×10^{13} cm^{-2}, while the lowest sheet resistivity, 15 Ω/□, was the result of a dose of 1×10^{15} cm^{-2}. For doses $\leq 1 \times 10^{13}$ cm^{-2}, the percentage activation and the mobility no longer increased with decreasing dose. It is believed that this is due to an excess of compensation in the Fe-doped InP ingot 25RH.

The results for Se^+ are shown in Fig. III-2 for two different Fe-doped InP samples implanted at 200°C and annealed at 750°C. The results on samples of ingot 25RH are very similar to those obtained on the same material with Si^+ (Fig. III-1). At a dose of 1×10^{14} cm^{-2}, 79 percent of the implanted Se is electrically active; at a dose of 1×10^{15} cm^{-2}, the sheet resistivity is 16 Ω/□; and for doses $\leq 1 \times 10^{13}$ cm^{-2} the percentage activation and mobility decrease with decreasing dose. On samples from crystal HPOZ9, the results are identical to those obtained on 25RH for doses $\geq 1 \times 10^{14}$ cm^{-2}. For low doses, however, the percentage activation increases with decreasing dose, apparently becoming greater than 100 percent for a dose of 1×10^{12} cm^{-2}.

TABLE III-1

SHEET HOLE CONCENTRATION (N_s) AND MOBILITY (μ_s) FOR BERYLLIUM, MAGNESIUM AND CADMIUM IMPLANTS IN InP

(All samples were implanted bare, encapsulated with PSG and annealed for 15 min. at the specified temperature.)

ION	ENERGY (keV)	DOSE (cm^{-2})	ANNEAL TEMP. (°C)	25°C IMPLANTS		200°C IMPLANTS	
				N_s (cm^{-2})	μ_s (cm^2/V-sec)	N_s (cm^{-2})	μ_s (cm^2/V-sec)
Be^+	50	1×10^{14}	700	3.5×10^{13}	83		
			725	2.9×10^{13}	100		
			750	3.3×10^{13}	81		
Mg^+	150	1×10^{14}	700	4.5×10^{13}	68		
			725	4.4×10^{13}	92	1.5×10^{13}	95
			750	5.2×10^{13}	83		
Cd^+	400	1×10^{14}	700	4.3×10^{12}	47	2.3×10^{13}	69
			725				
			750	1.6×10^{13}	90	3.7×10^{13}	91

This is consistent with the above-mentioned observation that heated and annealed samples of this crystal showed n-type surface layers even when unimplanted. The variations for low doses between different Fe-doped InP ingots are similar to those observed between Cr-doped GaAs ingots[14-16] and are currently under further investigation.

Ions of Cd^+, Mg^+, and Be^+ were employed to create p-type layers. Fe-doped (25RH) substrates were used exclusively, except for a few Mg implants into n-type material. Table III-1 lists the pertinent results. For samples implanted with 1×10^{14} cm^{-2} Cd^+, higher sheet hole concentrations were observed when the implants were carried out at 200°C. This is probably due to the lower residual n-type damage obtained when using heated substrates, in agreement with the Kr^+ results. Note that the concentration also increased with anneal temperature, reaching 3.7×10^{13} cm^{-2} with a mobility of 91 cm^{-2}/V-sec for a 200°C implant annealed at 750°C for 15 min.

For Mg^+ ions the results are the reverse of those for Cd^+, with the sheet hole concentration for a 1×10^{14} cm^{-2} implant being higher on samples implanted at room temperature than 200°C. Furthermore, there was not as significant an increase in N_S with anneal temperature as observed for Cd^+. The highest sheet concentration, 5.2×10^{13} cm^{-2}, was observed on a sample implanted with 1×10^{14} cm^{-2} Mg^+ and annealed at 750°C. For still higher Mg^+ doses ($\geq 3 \times 10^{14}$ cm^{-2}), the measured sheet concentrations were approximately the same for room temperature and 200°C implants and were smaller than that obtained for 1×10^{14} cm^{-2} room-temperature implants. These results and the reasons for their difference from those for Cd^+ are not presently understood. Samples implanted at 77 K gave results identical to those obtained at room temperature, and similar results were also obtained for implants made into n-type substrates ($n \approx 4 \times 10^{16}$ cm^{-3}).

A limited number of Be^+ implants were made and only into room-temperature substrates. The sheet hole concentrations of samples implanted with 1×10^{14} cm^{-2} Be^+ at 50 keV did not vary much for anneal temperatures between 700° and 750°C and were about 3×10^{13} cm^{-2}.

J. P. Donnelly
C. E. Hurwitz

B. FE^+ IMPLANTED HIGH-RESISTIVITY LAYERS IN InP

The ability to selectively form high-resistivity layers in GaAs and related Ga-based III-V compounds by proton bombardment[17-26] or oxygen ion implantation[27] has been used to advantage in the fabrication of a wide variety of microwave and electrooptical devices. (For a summary of applications see, for example, Ref. 28 or 29.) More recently, this technique has been used successfully with InP to fabricate stripe-geometry InP/InGaAsP lasers.[30,31] In InP, however, it was observed that, although proton bombardment can result in increases of the resistivity of p-type material to greater than 10^8 Ω-cm, the maximum observed resistivity of proton bombarded n-type InP was approximately 10^3 Ω-cm (Refs. 32 and 33). In an effort to obtain higher resistivities in n-type material, we have investigated the implantation of Fe, an impurity which is known to result in high-resistivity InP when used as a dopant during growth of bulk crystals.[34] We have found that the implantation of Fe^+ followed by a suitable anneal can increase the resistivity of n-type InP to at least 10^7 Ω-cm. In this section, we will discuss the implantation and anneal procedures and present our initial experimental results.

The n-InP samples used in these experiments were cut from (111)-oriented crystals grown by the liquid encapsulation Czochralski technique and had carrier concentrations of (4 to 7) × 10^{16} cm^{-3} or ≈ 1 × 10^{18} cm^{-3}. After polishing, the samples were etched in a 1:1:6:1 solution of HAc:$HClO_4$:HNO_3:HCl (Ref. 8). Implants of Fe^+ were performed at both room temperature and 200°C with the samples tilted in reference to the ion beam to minimize channeling. A multiple-energy implantation schedule was used on all samples in an attempt to create a layer with a uniform Fe concentration. The range and range straggling statistics were obtained using a computer program developed by Johnson and Gibbons[35] and based on LSS theory.[36] The multiple-dose schedule selected was N at 400 keV, 0.36 N at 190 keV, 0.18 N at 90 keV, and 0.1 N at 40 keV, where N is in units of cm^{-2}.

Following implantation, each sample was encapsulated with 2500 Å of pyrolytic phosphosilicate glass deposited at 250°C by the technique described in part A of this section. Samples were then annealed in flowing nitrogen. In preliminary experiments, the anneal temperature was varied from 650° to 750°C and the anneal time from less than 1 min. (pulse heating) to 15 min. Although good results were obtained over a rather broad range of anneal temperatures and times, an anneal at 725°C for 15 min. generally resulted in layers of the highest resistivity and was used almost exclusively in subsequent experiments. As discussed below, however, the anneal schedule does influence the amount of diffusion of the implanted Fe and may have to be modified for specific applications.

After annealing, holes were opened in the PSG, through which 5- to 15-mil-diameter gold contacts were plated on the Fe-implanted layers. Illumination from a microscope lamp was used during plating to achieve sufficient electrical conductivity in the insulating layer. A large-area gold back contact, with a measured contact resistance of a few ohms, was plated on the n-type substrate. To evaluate the effects of the Fe-ion implantations, the current-voltage and capacitance-voltage characteristics as well as the equivalent zero-bias parallel resistance and capacitance of the Au/Fe-implanted InP/n-substrate structures were measured.

For material with an initial carrier concentration in the range of (4 to 7) × 10^{16} cm^{-3}, multi-energy Fe implants with doses corresponding to N = 5 × 10^{12} to 1 × 10^{14} cm^{-2} were investigated. Maximum zero-bias resistances (RA > 6 × 10^3 Ω-cm^2) were obtained for N = (2 to 6) × 10^{13} cm^{-2}. For material with an initial concentration of about 10^{18} cm^{-3}, a dose of N ≈ 4 × 10^{14} cm^{-2} gave the highest resistance. However, the value of this resistance was typically 5 to 10 times lower than that obtained in the more lightly doped material. Figure III-3

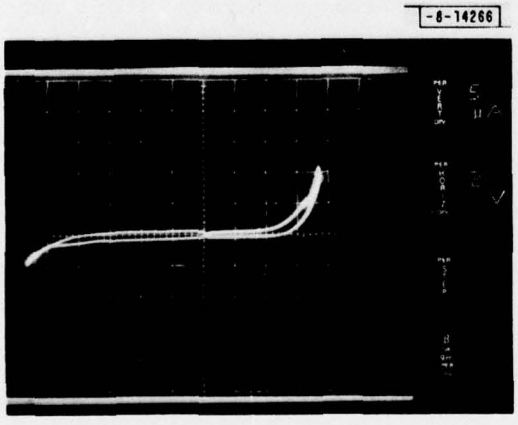

Fig. III-3. Current-voltage characteristics of 5-mil-diameter gold contact on n = 6 × 10^{16} cm^{-3} InP after a room-temperature multi-energy Fe^+ implantation with N = 4 × 10^{13} cm^{-2} (see text) followed by a 725°C, 15-min. anneal.

shows the current-voltage characteristics of a 5-mil-diameter Au contact on an InP sample with an initial concentration of 6×10^{16} cm^{-3}, which was implanted with a multi-energy Fe schedule with N = 4×10^{13} cm^{-2} and annealed at 725°C for 15 min. The difference in breakdown voltage between the forward direction (top contact positive) and the reverse direction is at least partially due to the increase of the depletion layer thickness in the n-type substrate with increasing reverse bias. The zero-bias resistance is greater than 50 MΩ, and the zero-bias capacitance is 1.87 pF, from which one deduces that the high-resistivity layer is about 0.8 μm thick and has an average resistivity of 6×10^{7} Ω-cm.

The 0.8-μm depth of the implanted Fe^{+} ions is much greater than expected from LSS theory[36] for the implant schedule used. Furthermore, samples implanted with the same schedule but annealed at lower temperatures exhibit higher capacitances and presumably have thinner high-resistivity layers. For example, 5-mil-diameter Au contacts on a sample annealed at 650°C had capacitances of 2.70 pF, while those on a sample annealed at 700°C had capacitances of 2.37 pF. In the range of 1 to 15 min., increasing anneal times also resulted in decreased values of capacitance. These results indicate that considerable diffusion of the implanted Fe must be taking place during the post-implantation anneal. Samples implanted at 200°C also exhibited higher capacitances than similar samples implanted at room temperature, indicating that the Fe diffusion can be reduced by implanting into heated substrates.

Depth profiles of effective carrier concentrations in the layers were obtained from capacitance-voltage measurements. The effective carrier concentration, n_{eff}, was calculated using the well-known relations

$$n_{eff}(x) = \frac{C^3}{q\epsilon A^2(-\frac{dC}{dV})} \quad \text{and} \quad x = \frac{\epsilon A}{C}$$

where $n_{eff}(x)$ is the effective carrier concentration at depth x, C is the capacitance, A is the area of the diode, V is the applied voltage (assumed positive in the reverse direction), q is the electronic charge, and ϵ is the static dielectric constant for InP. Figure III-4 shows the results of measurements made at 500 kHz on two samples, one implanted at room temperature and the other implanted at 200°C with the same multi-energy Fe-implant schedule (N = 4×10^{13} cm^{-2}). Both samples were annealed at 725°C for 15 min. Also shown is the as-implanted Fe profile expected from LSS theory.[36] In agreement with the zero-bias capacitance measurements, the low carrier concentration region (high-resistivity region) of the room-temperature implant is ≈0.8 μm thick. On the other hand, the high-resistivity region in the sample implanted at 200°C is only ≈0.55 μm, which is closer to the calculated profile, again indicating that diffusion during anneal is less for the hot implants.

Both samples shown in Fig. III-4 appear to have an anomalous carrier concentration peak at the edge of the high-resistivity region, similar to those which have been observed in proton-bombarded GaAs.[18,21] We do not believe that these peaks are real "donor peaks," and we suggest the following alternative explanation. Figure III-5 is a representation of the band diagram of our structure, assuming that the Fe acts as a simple deep acceptor near the middle of the gap and that the Fermi level at the surface is pinned about one-third of the way down from the conduction-band edge. For the implanted layer to be high resistivity, the Fermi level must be near the center of the gap, which in turn requires that the implanted Fe concentration must be greater than about twice the donor concentration. This requirement also makes the "effective

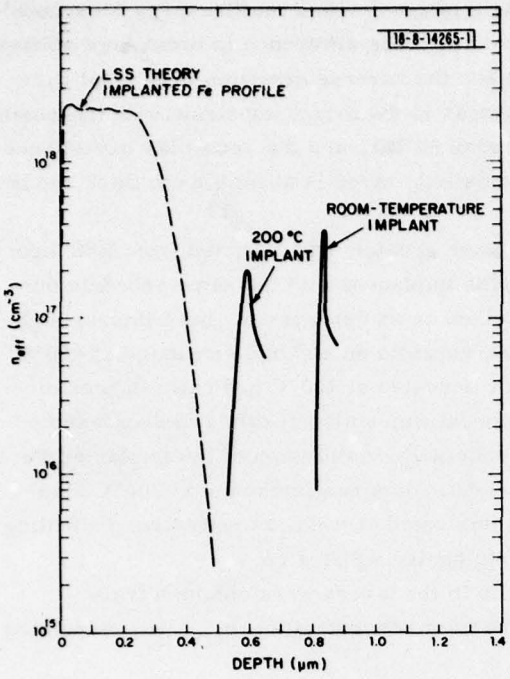

Fig. III-4. Effective carrier concentration vs depth obtained from capacitance-voltage measurements for two InP ($n = 6 \times 10^{16}$ cm^{-3}) samples after a multi-energy Fe^+ implant and a 725°C 15-min. anneal. One sample was implanted at room temperature and the other at 200°C.

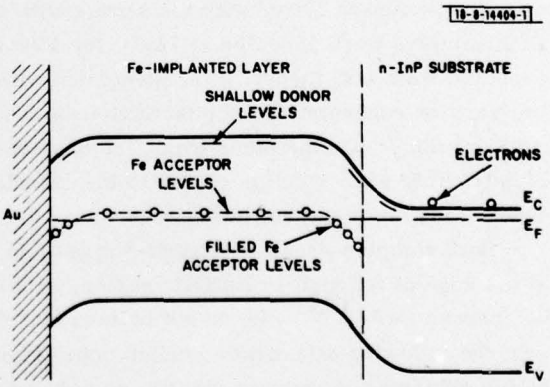

Fig. III-5. Representative band diagram of Fe-implanted n-type InP indicating the filing of excess Fe levels at the interface.

Debye length" in the high-resistivity implanted region short enough so the space-charge regions at the substrate interface and at the Au contact extend only a short distance into the implanted layer. Due to band-bending near the interface, the Fe levels in this region will drop below the Fermi level, and in equilibrium the excess Fe levels will be filled. Although a detailed analysis of this model has not yet been completed, we believe that the charging and discharging of the Fe levels with a change in applied bias[37] can result in what appears to be a peak in the carrier concentration. Emission from deep levels has also been proposed[21] to explain similar results in proton-bombarded GaAs.

In addition to the implants into bare n-InP samples, we have made some implants through 500 Å of PSG or an anodic oxide. Although the results were not as reproducible as those for samples implanted bare, high-resistivity layers with $\rho \geq 10^7$ Ω-cm were obtained. The depth of the high-resistivity region was approximately 0.66 μm for a room-temperature implant ($N = 4 \times 10^{13}$ cm^{-2}) made through a 500-Å layer of PSG.

J. P. Donnelly
C. E. Hurwitz

C. GUARDED InP PHOTODIODES

Initial attempts to fabricate guarded photodiodes in InP by means of ion implantation have led to unanticipated difficulties. The goal is to create p-n junctions by implanting p-type layers of Cd or Mg into n-type InP substrates and to then create high-resistivity guard rings by implantation of Fe (see parts A and B of this section). During annealing to remove the radiation damage introduced by the implantation, the implanted Cd and Mg appeared to diffuse much more rapidly than expected, resulting in p-n junctions which were deeper than the guard rings. As a result, little or no guarding was achieved and the diodes showed poor breakdown characteristics.

Efforts to reduce this diffusion of the acceptors by implanting them at elevated temperatures and/or by the co-implantation of P^+ were initiated. This latter technique has been shown by others[38,39] to be effective in reducing diffusion of Cd and Zn in GaAs. Initial results of these experiments were inconclusive. This work has been temporarily suspended while attention is focused on the recently successful diffused GaInAsP/InP avalanche photodiodes (see Sec. II).

C. E. Hurwitz
J. P. Donnelly

REFERENCES

1. Semiannual Technical Summary on Electrooptical Devices, Lincoln Laboratory, M.I.T. (31 March 1977), p. 1, DDC AD-A046483.
2. T. Yamamoto, K. Sakai, and S. Akiba, Electron. Lett. 13, 142 (1977).
3. T. P. Pearsall and R. W. Hopson, Jr., J. Electron. Mater. 7, 133 (1978).
4. H. H. Wieder, A. R. Clawson, and G. E. McWilliams, Appl. Phys. Lett. 31, 468 (1977).
5. G. E. Stillman, C. M. Wolfe, J. A. Rossi, and J. P. Donnelly, Appl. Phys. Lett. 25, 671 (1974).
6. D. E. Davies, T. K. Kennedy, and L. F. Lowe, Electron. Lett. 11, 462 (1975).
7. Semiannual Technical Summary on Electrooptical Devices, Lincoln Laboratory, M.I.T. (31 March 1977), p. 10, DDC AD-A046483.
8. R. Becker, Solid-State Electron. 16, 1241 (1973).
9. J. P. Donnelly, W. T. Lindley, and C. E. Hurwitz, Appl. Phys. Lett. 27, 41 (1975).
10. C. O. Bozler, J. P. Donnelly, R. A. Murphy, R. W. Laton, R. W. Sudbury, and W. T. Lindley, Appl. Phys. Lett. 29, 123 (1976).
11. J. P. Donnelly, in Gallium Arsenide and Related Compounds (St. Louis) 1976, L. F. Eastman, Ed. (The Institute of Physics, Bristol and London, 1977), p. 166.
12. B. J. Baliga and S. K. Ghandhi, in Tech. Digest Intl. Electron Device Meeting, Washington, D. C., 1973 (IEEE, New York, 1973), p. 256.
13. L. J. van der Pauw, Philips Research Rep. 13, 1 (1958).
14. J. P. Donnelly, C. O. Bozler, and W. T. Lindley, Solid-State Electron. 20, 273 (1977).
15. W. Kellner, H. Kniepkamp, D. Ristow, M. Heinzle, and H. Boroffka, Solid-State Electron. 20, 459 (1977).
16. C. A. Stolte, in Tech. Digest Intl. Electron Device Meeting, Washington, D.C., 1975 (IEEE, New York, 1975), p. 585.
17. K. Wohlleben and W. Beck, Z. Naturf. 21A, 1057 (1966).
18. A. G. Foyt, W. T. Lindley, C. M. Wolfe, and J. P. Donnelly, Solid-State Electron. 12, 209 (1969).
19. J. C. Dyment, J. C. North, and L. A. D'Asaro, J. Appl. Phys. 44, 207 (1973).
20. B. R. Pruniaux, J. C. North, and G. C. Miller, in Proc. Int. Conf. on Ion Implantation in Semiconductors, 1971 (Springer-Verlag, Berlin, 1971), p. 212.
21. H. Haradu and M. Fujimoto, in Proc. Int. Conf. on Ion Implantation in Semiconductors, 1974 (Plenum, New York, 1975), p. 73.
22. J. P. Donnelly and F. J. Leonberger, Solid-State Electron. 20, 183 (1977).
23. J. D. Speight, P. O'Sullivan, P. A. Leigh, N. McIntyre, K. Cooper, and J. O'Hara, in Gallium Arsenide and Related Compounds (Edinburgh), 1976 (The Institute of Physics, London, 1977, Conf. Ser. 33a), p. 275.
24. J. C. Dyment, L. A. D'Asaro, J. C. North, B. I. Miller, and J. E. Ripper, Proc. IEEE 60, 726 (1972).
25. P. N. Favennec and D. Diguet, Appl. Phys. Lett. 23, 546 (1973).
26. P. M. Spitzer and J. C. North, J. Appl. Phys. 44, 214 (1973).
27. P. N. Favennec, J. Appl. Phys. 47, 2532 (1976).

28. P. L. F. Hemment, in Applications of Ion Beams to Materials, 1975 (The Institute of Physics, London, 1976, Conf. Ser. 28), p. 44.

29. J. P. Donnelly, in Gallium Arsenide and Related Compounds (St. Louis), 1976 (The Institute of Physics, London, 1977, Conf. Ser. 33b), p. 166.

30. J. J. Hsieh, J. A. Rossi, and J. P. Donnelly, Appl. Phys. Lett. 28, 709 (1976).

31. J. A. Rossi, J. J. Hsieh, and J. P. Donnelly, in Gallium Arsenide and Related Compounds (St. Louis), 1976 (The Institute of Physics, London, 1977, Conf. Ser. 33b), p. 303.

32. J. P. Donnelly and C. E. Hurwitz, Solid-State Electron. 20, 727 (1977).

33. Semiannual Technical Summary on Electrooptical Devices, Lincoln Laboratory, M.I.T. (31 March 1977), p. 5, DDC AD-A046483.

34. O. Mizuno and H. Watanabe, Electron. Lett. 11, 118 (1975).

35. W. Johnson and J. F. Gibbons, Projected Range Statistics in Semiconductors (Stanford University Bookstore, Stanford, Calif., 1970).

36. J. Lindhard, M. Scharff, and H. Schiott, K. Dan Vidensk Selsk, Mat.-Fys. Medd. 33, 1 (1963).

37. For the band structure shown in Fig. III-5, this is essentially a single-carrier problem and is similar to single-injection with traps. See, for example, M. A. Lampert and R. B. Schilling, in Semiconductors and Semimetals, Vol. 6, R. K. Willardson and A. C. Beer, Eds. (Academic Press, New York, 1970), p. 1.

38. A. A. Gavrilov, G. A. Katchurin, N. B. Pridachin, and C. S. Smirnov, Sov. Phys.-Semiconductors 8, 1455 (1975).

39. K. Aoki, K. Gamo, K. Masuda and S. Namba in Ion Implantation in Semiconductors, 1976, edited by F. Chernow, J. A. Borders, and D. K. Brice, (Plenum, New York, 1977), p. 123.

UNCLASSIFIED

SECURITY CLASSIFICATION OF THIS PAGE *(When Data Entered)*

REPORT DOCUMENTATION PAGE		READ INSTRUCTIONS BEFORE COMPLETING FORM
1. REPORT NUMBER ESD-TR-78-28	2. GOVT ACCESSION NO.	3. RECIPIENT'S CATALOG NUMBER
4. TITLE *(and Subtitle)* Electrooptical Devices		5. TYPE OF REPORT & PERIOD COVERED Semiannual Technical Summary 1 April – 30 September 1977
		6. PERFORMING ORG. REPORT NUMBER
7. AUTHOR(s) Ivars Melngailis and Arthur G. Foyt, Jr.		8. CONTRACT OR GRANT NUMBER(s) F19628-76-C-0002
9. PERFORMING ORGANIZATION NAME AND ADDRESS Lincoln Laboratory, M.I.T. P.O. Box 73 Lexington, MA 02173		10. PROGRAM ELEMENT, PROJECT, TASK AREA & WORK UNIT NUMBERS Program Element Nos. 62702F and 61102F Project No. 261104
11. CONTROLLING OFFICE NAME AND ADDRESS Rome Air Development Center Griffiss AFB, NY 13440		12. REPORT DATE 30 September 1977
		13. NUMBER OF PAGES 28
14. MONITORING AGENCY NAME & ADDRESS *(if different from Controlling Office)* Electronic Systems Division Hanscom AFB Bedford, MA 01731		15. SECURITY CLASS. *(of this report)* Unclassified
		15a. DECLASSIFICATION DOWNGRADING SCHEDULE

16. DISTRIBUTION STATEMENT *(of this Report)*

Approved for public release; distribution unlimited.

17. DISTRIBUTION STATEMENT *(of the abstract entered in Block 20, if different from Report)*

18. SUPPLEMENTARY NOTES

None

19. KEY WORDS *(Continue on reverse side if necessary and identify by block number)*

electrooptical devices	proton bombardment	ion implantation
avalanche photodiodes	double-heterostructure	GaInAsP/InP lasers

20. ABSTRACT *(Continue on reverse side if necessary and identify by block number)*

Considerable progress has been made toward the achievement of the current objectives of the electrooptical device program. These goals are: (1) to perform life tests on GaInAsP/InP double-heterostructure (DH) diode lasers operating in the 1.0- to 1.3-micron wavelength region and analyze the degradation mechanisms, and (2) to fabricate and study avalanche photodiodes of similar composition GaInAsP operating in the same wavelength region.

Life tests of CW, room-temperature GaInAsP/InP DH lasers have continued with a total of 13 devices examined in some detail. Eleven of the lasers have operated for over 2000 hours, with

DD FORM 1 JAN 73 1473 EDITION OF 1 NOV 65 IS OBSOLETE

UNCLASSIFIED

SECURITY CLASSIFICATION OF THIS PAGE *(When Data Entered)*

20. ABSTRACT (Continued)

the longest-lived operating 7700 hours before failure. End-face contamination problems have apparently been reduced and other mechanisms for degradation, both of external and internal nature, are under study.

CW operation of the DH GaInAsP/InP lasers has been demonstrated at temperatures up to 50°C. The pulsed threshold was found to increase with temperature as $J_{th} = J_o \exp(T/T_o)$ with $T_o \approx 75$°C and J_o a constant. Over the temperature range 10°C < T < 50°C, the temperature dependence of the wavelength was approximately linear with $\Delta\lambda/\Delta T \approx 3.2$ Å/°C.

The pulse response and modulation characteristics of GaInAsP/InP lasers have also been investigated. Clean output pulses with risetimes of less than 250 psec, pulse modulation at 200 megapulses/sec, and pulse-position modulation at a 100-Mbit/sec rate have been achieved. Modulation rates in the GHz range should be attainable.

Avalanche diodes with response from 0.9 to 1.3 μm have been successfully fabricated in GaInAsP/InP double-heterostructure configurations. Uniform avalanche gains in excess of 12, risetimes of 200 psec or less, and low bias quantum efficiencies of 45 percent have been measured.

Implantation of ions of Se^+ and Si^+ has been used to create n-type layers in InP. With both ions, sheet resistivities of 15 to 16 Ω/□ have been achieved with electrical activations of nearly 80 percent over a wide range of doses. P-type layers were created with Cd^+, Mg^+, and Be^+, with initial studies concentrating on the effects of varying implant and anneal temperatures. Diffusion of these p-type dopant ions during annealing has been found to be more rapid than expected.

Studies of the implantation of Fe^+ shows that high-resistivity layers ($\rho > 10^7$ Ω-cm) can be created in n-type InP. Depth profiles indicate a relatively rapid diffusion of the Fe during anneal. An apparent anomalous donor peak at the edge of the high-resistivity region has been tentatively explained by a model involving the charging and discharging of the Fe levels.